Available online at www.sciencedirect.com
SCIENCE DIRECT
Journal of Sound and Vibration 292 (2006) 1–20
JOURNAL OF SOUND AND VIBRATION
www.elsevier.com/locate/jsvi

Experimental analysis of brake squeal noise on a laboratory brake setup

Oliviero Giannini[a,*], Adnan Akay[b], Francesco Massi[a]

[a]*Department of Mechanics and Aeronautics, University of Rome "la Sapienza", Via Eudossiana, 18-00184 Rome, Italy*
[b]*Mechanical Engineering Department, Carnegie Mellon University, Pittsburgh, PA, USA*

Received 14 December 2004; received in revised form 14 April 2005; accepted 31 May 2005
Available online 7 February 2006

Abstract

The present paper is the first of two papers dealing with brake squeal instability. An experimental setup is specifically designed for this purpose and is characterized by a simple design to aid measurements and modeling. This first paper describes the experimental setup called "laboratory brake" and presents the measurements performed on it to characterize its dynamical behavior and its squeal behavior. The tests are aimed at identifying the key parameters controlling the squeal phenomenon that are necessary to build a model of the setup. The experimental analysis on squeal presented here identifies several characteristics that lead to instabilities and correlates them with the operating parameters as well as with the dynamic behavior of the system. Measurements also highlight that the pad dynamics have a key role in the selection of the squealing modes at one of the out-of-plane eigenfrequency of the system. Finally, the experimental results provide a better understanding of the physics of the squeal mechanism and suggest guidelines to build a representative model of the setup.

1. Introduction

The present paper is the first of two papers on brake squeal noise. The study describes the characteristic features of squeal sound emissions and correlates such features to the dynamic behavior of a brake using a specially designed apparatus. In this first paper, the description of the setup as well as the measurements performed to characterize its dynamic behavior under squeal conditions is presented. A second paper will introduce a reduced-order model able to describe the setup behavior and predict the squeal occurrence.

Brake squeal refers to the high-frequency sound emissions from a brake that are generated during the braking phase and characterized by a periodic or harmonic spectrum. This phenomenon is common to both drum and disc configurations and concerns both train and automotive brakes. Therefore, the geometry and the dimension of brakes can vary widely, thus leading to very different sets of squeal frequencies and associated modes.

Brake squeal continues to be a major concern for car companies and a robust procedure for a "squeal-free" design is still under investigation. Kinkaid et al. [1], in their extensive review of brake squeal literature,

*Corresponding author. Fax: +39 64881759.
E-mail address: oliviero.giannini@uniroma1.it (O. Giannini).

0022-460X/$ - see front matter
doi:10.1016/j.jsv.2005.05.032

concluded that "despite a century of developing disc brake systems, disc brake squeal remains a largely unresolved problem", highlighting how, even if a good understanding of the problem has been achieved, design solutions are not yet ready.

In over 70 years of research on brake squeal, many experimental studies report detailed aspects of squeal behavior. Among the earlier ones, Mills [2], Fosberry and Holubecki [3,4], and Spurr [5] tried to correlate experimental results with their models, while North [6] was the first who worked extensively on a commercial brake apparatus, correlating experimental results with his model.

In 1989, Nishiwaki et al. [7] presented an experimental study performed with the dual pulse holographic interferometer (DPHI) technique: they compared the squealing deformed shapes with the modes of the stationary rotor and found the two to be very close to each other. Fieldhouse and Newcomb [8,9], using a holographic technique, observed instances when the deformed shapes are not stationary but had traveling wave components.

In 2001, Denou and Nishiwaki [10] presented a study on low-frequency squeal from a modified disc brake. They reduced the contact area between pads and disc and between the cylinders and the backplates to correlate the results with their model. They found that the deformed shapes that develop during squeal consist of a combination of many bending modes of the uncoupled rotor.

Experimental investigation of brake squeal noise is non-trivial for the same reasons that brake squeals in automobiles occur seemingly randomly. Just as it is not possible yet to design a squeal-free brake, for the same reason it is not possible to design functional brakes that squeal all the time. Because every research group that experimentally investigates brake squeal has its own setup, a specific model of rotor, caliper, pads (sometimes slightly modified for instrumentation accessibility), makes it difficult to exchange and compare meaningful results.

It is generally accepted that one of the main difficulties encountered in studying brake squeal is due to the high complexity of the brake apparatus: in fact such complexity along with the everpresence of dispersion of data in experimental studies are the reasons for the variety of suggestions and explanations regarding brake squeal proposed throughout the years.

The physics of squeal occurrence and the related theoretical models are described in many papers: among the first studies on brake squeal, Mills [2] and Fosberry and Holubecki [3,4] tried to correlate the occurrence of squeal during experiments with a negative slope of the friction coefficient-relative velocity curve ($\mu - v_r$), while Spurr [5] proposed his sprag-slip theory, followed later by Earles et al. [11,12] and Jarvis and Mills [13]. In 1972, North [6,14] published the first experimental work on a real brake apparatus and correlated his measurements results with a model. More recently Popp and Stelter [15], and Rudolph and Popp [16], correlate the squeal to stick-slip vibration and chaos, Mottershead [17], and Chan et al. [18], equate the squeal to two different set of instabilities: the first set produces instabilities at sub-critical parametric resonances; the second set, caused by the friction interaction between disc and pad, destabilizes the backwards waves of all the modes with nodal diameters.

In this paper, to avoid the difficulties arising from the complexity of the brake we propose a simplified experimental rig, able to reproduce the main features of a commercial disc brake but with a more simple geometry which allows for a simplified modeling. We called this setup "the laboratory brake".

In the past years, based on the assumption that simplifying the brake apparatus it is necessary in order to obtain reliable data during tests, many research groups: Akay et al. [19], Tucinda et al. [20,21], Allgaier et al. [22,23], Tarter [24], involved in the study of the brake squeal phenomenon, conducted extensive analyses of the beam-on disc setup.

The study of the squeal events using the beam-on-disc setup [19] allowed for modeling the friction interaction between a beam and a disc that leads to the unstable behavior.[1] The developed model was able to predict the conditions necessary for the squeal event; however, such good results could not be obtained with a similar methodology applied to the analysis of a complex disc brake apparatus.

[1]In literature, squeal noise is usually correlated to unstable vibration. Actually, the instability leads to a limit cycle characterized by large vibration amplitude.

Thus, we believe that there is still the need for an experimental setup that must be considered as a ''trait d'union'' between the beam-on-disc setup and a commercial brake and this is the aim of the laboratory brake presented in this paper.

2. Characteristics of the laboratory brake

The design of the laboratory brake setup has evolved over several years with the aim of simulating a real brake as closely as possible, while maintaining some basic qualities necessary for an investigation tool that are summarized as follows.

Measurability: The main purpose of the test rig is to correlate generation and characteristics of squeal sounds to the apparatus dynamics; therefore the dynamic behavior of the lab-brake parts must be measured appropriately to retrieve information about both the system as a whole and its components. Lab brake must be designed so that each of its components can be accessible by instrumentation.

Operational parameters: Operational parameters such as normal load, relative velocity, geometrical configuration of the setup, should be measurable and controllable during experiments; it is also important that such parameters correspond to the real brake operational parameters.

Contact: The pads used in the laboratory brake are made by machining commercial brake pads. The contact area between a pad and disc can be adjusted by changing the pad length. Measurements must be able to correlate the squeal tendency of the setup to the material properties and geometry of the pad.

Dynamic behavior: To use the lab-brake as an investigative tool to correlate the dynamic behavior of the system with the squeal characteristics, the dynamics of the setup must be adjustable to study how changes affect squeal.

Aim: The lab-brake is a setup aimed at studying the squeal phenomenon in disc brakes; therefore the brake pads are in contact with the face of the disc.

Such features of the setup make the laboratory brake a suitable tool to study the squeal phenomenon, but the overall quality of the laboratory brake is its ability to generate squeal events easily, robustly and consistently.

An ''easy to squeal'' setup allows for the measurement of many different squeal behaviors and producing a variety of data under controlled conditions.

The tests described later also show the robustness of the setup such that when a squeal condition is attained, small changes in the operating parameters do not affect the squeal behavior.

Consistency implies reproducibility of the squeal conditions: when a set of parameters produces a certain squeal behavior, it is possible to always reproduce that specific behavior by just rolling back the parameters.

The beam-on-disc setup [19–24] fulfills these criteria and reproduces many squeal conditions with these qualities. Unfortunately, the increased complexity of the laboratory brake with respect to the beam-on-disc setup involves a decrease in robustness, consistency and facility for the squeal generation. In the case of the lab-brake, the increased number of parameters required to describe the squeal behavior it produces, increases the difficulty of defining the boundaries of a particular squeal condition.

The laboratory brake setup should be considered as an experimental bridge between the beam-on-disc, which represents the upper limit in reliability, and a commercial disc brake, which represents the upper limit in complexity.

The design described here offers the best compromise between these two limits.

If not noted otherwise, the most of the results presented in this work are obtained by the Laboratory Brake V.2.3,[2] the latest of five different setups that were designed and constructed for this study. The previous setup is characterized by disc of different dimension and material but with the same characteristics. Therefore, the results obtained from these setups present slightly different eigenfrequencies and squeal occurrences.

[2]Extensive description of the setup along with the main differences between them can be found in Ref. [25].

2.1. Description of the experimental rig

The laboratory brake consists of a stainless steel disc with nominal diameter of $D = 360\,\text{mm}$, and a thickness of 19 mm. The disc is held by two bearings that are attached to an aluminum frame fixed to a table. An electric motor (750 W of power) rotates the disc. The motor speed can be changed and monitored by a controller. Between the motor and the disc, a speed reducer (1/34 speed ratio) and two pulleys connected by a belt (1/4 speed ratio) are inserted for a total speed ratio of 1/136. The diameter of the pulleys can be changed to increase the speed range of the disc.

Fig. 1 shows the schematic top view of the setup. Two steel beams (A and B) act as a caliper that hold the brake pads (C and D), each of which has an area of $1\,\text{cm}^2$. Two bolts (E and F) are used to apply and adjust the normal load, which is measured by load cells. Two thin aluminum plates (G and H) hold the beams in the vertical direction fairly rigidly while allowing the beams to "float" in the horizontal direction. Two supports (I and L) connect the aluminum plates to the table.

The two beams that function as the brake caliper can rotate with respect to the disc plane, simulating a misalignment angle α of the pads, also called angle of attack.

Fig. 2 shows a front picture of the experimental setup.

The design attributes of the setup are such that:

- the geometry of the caliper is extremely simple, making it easy to model;
- the measurement of normal load is not direct but easily calculated from the measurement of the load applied by the bolt;

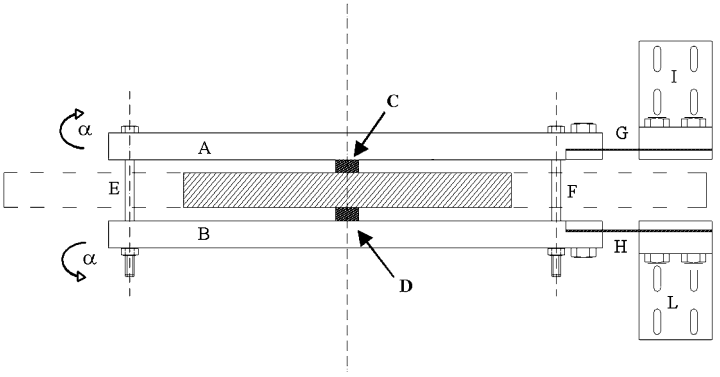

Fig. 1. Schematic top view of the lab-brake.

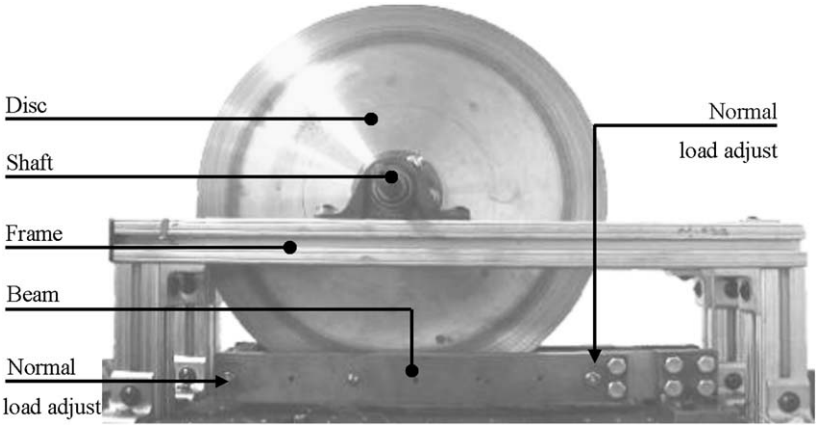

Fig. 2. Front view of the lab-brake.

- the caliper can float: therefore, small misalignments between the shaft and the disc plane do not cause large variations of the normal load during the rotation of the disc; the effects of disc thickness variation (DTV) on normal load can be easily reduced by machining the surface of the disc periodically;
- the setup can host pads with different dimensions and geometry;
- the angle of attack of the beam can be adjusted and measured.

2.2. Dynamic behavior of the laboratory brake

This section discusses the dynamic behavior of the laboratory brake: Tables 1[3] and 2 display the results of an experimental modal analysis (EMA) performed on the laboratory brake components, when the disc and the beams are not in contact. We will refer to this condition as "uncoupled conditions", while we refer to the tests performed on the assembled components of the laboratory brake as "coupled conditions".

The disc modes (n, m) is characterized by n nodal circumferences and m nodal diameters. The disc is axially symmetric; therefore the modes of the disc are generally repeated modes.

The test results for the uncoupled case provide a reference behavior for the laboratory brake as well as the data needed to model the setup.

The EMA performed considered only the bending modes of the disc and the beam. We refer to the displacement direction of these modes as the "out-of plane" direction. We refer to the nominal direction of the relative velocity between disc and beam as the "in-plane" direction.

The aim of this study is to identify any correlation between squeal generations and the dynamic behavior of the brake and its components. The most important goal of this study is to determine which characteristics of the interaction between disc and caliper modes lead to an unstable behavior.

This goal is the main reason for choosing small pads for the setup and applying low normal pressure between disc and pads so that their coupled behavior can be easily explained as the sum of those of the separate components. In fact, this choice implies weak coupling between modes and, therefore, the coupled deformed shapes are similar to the brake component modes measured under uncoupled conditions. It is important to note that the setup is characterized by its modes. Reference to coupled (n, m) mode of the disc implies that the coupled system is vibrating with a displacement similar to the uncoupled (n, m) mode of the disc.

The coupling between the disc and the beam modes increases when either the contact area (compared to the mode wave-length) or the contact pressure increases.

2.3. Coupled system

The first set of measurements to characterize the behavior of the coupled setup resulted from scanning the surface of the disc and the front beam with a laser vibrometer over a grid of 300 point, while exciting the structure with an impact hammer producing a bandwidth up to 12.5 kHz.[4]

The frequency response functions (FRFs) (Figs. 3 and 4) of the coupled system exhibit peaks that correspond to the uncoupled disc and beam modes, particularly where the beam and disc natural frequencies are far apart. These measurements form the basis for the following observations about the dynamic behavior of the coupled system:

- as a result of contact with the pads, the disc loses its axial symmetry and the modes of the disc with repeated eigenfrequencies split;
- between each pair of split modes of the disc, the one with lower frequency is characterized by a nodal line passing through the contact point and the one with the higher frequency has an antinode at the contact area;

[3]In the table appear a (1,1 +) mode of the disc. The mode with one nodal diameter is heavily coupled with the shaft vibration. Since the shaft has non-axi-symmetric constraints, such modes are not double even in free condition.

[4]See Appendix A, Table A1 for the scan parameters used in this test.

Table 1
Modal parameters of the disc

Mode	Frequency	Damping (%)	Mode	Frequency	Damping
(0,1)	709	2.60	(1,0)	3467	4.70
(0,2)	845	0.80	(0,5)	4660	0.03
(0,0)	1010	11.00	(1,2)	5100	0.54
(0,3)	1823	0.09	(0,6)	6426	0.03
(1,1)	2612	2.25	(1,3)	7174	0.19
(1,1 +)	2846	1.21	(0,7)	8378	0.02
(0,4)	3114	0.08	(1,4)	9541	0.05

Table 2
Modal parameters of the beam

Mode	Frequency (Hz)	Damping (%)
1	877	0.90
2	2180	1.41
3	4260	0.33
4	6750	0.30
5	9560	0.21

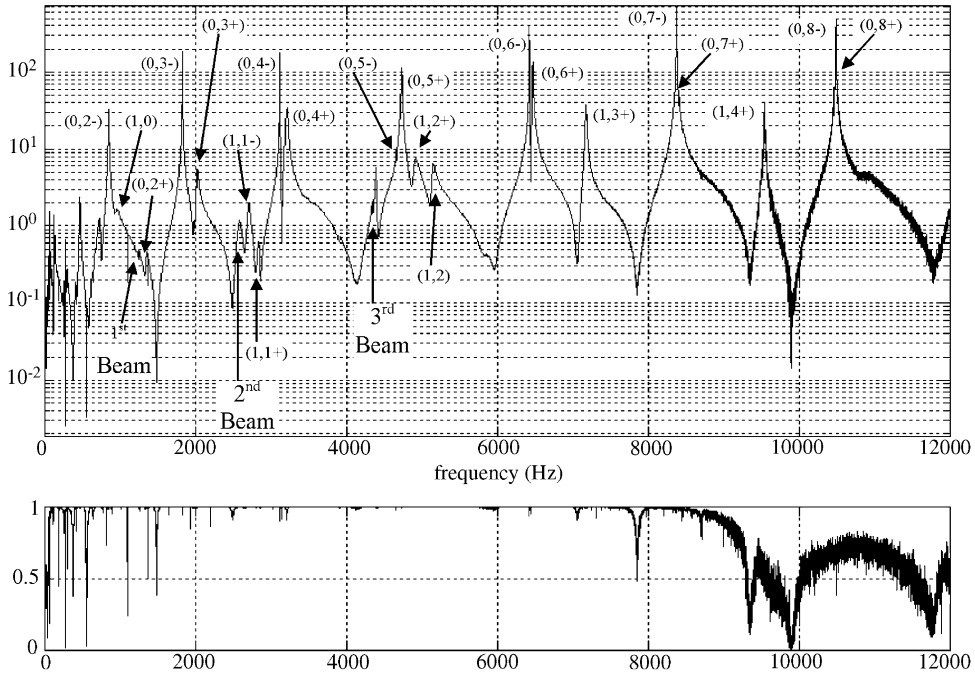

Fig. 3. Frequency response function and coherency function of the coupled system.

- the lower frequency mode of the split pair has a frequency close to (generally a few Hertz higher) the frequency of the same mode under uncoupled conditions. The second of the split modes has a higher frequency, which increases with the normal load;
- the frequency split of the disc modes with one or more nodal circumference ($n>0$) is only a few hertz, much less than the (0,m) modes and are not usually detected in the measurements presented;

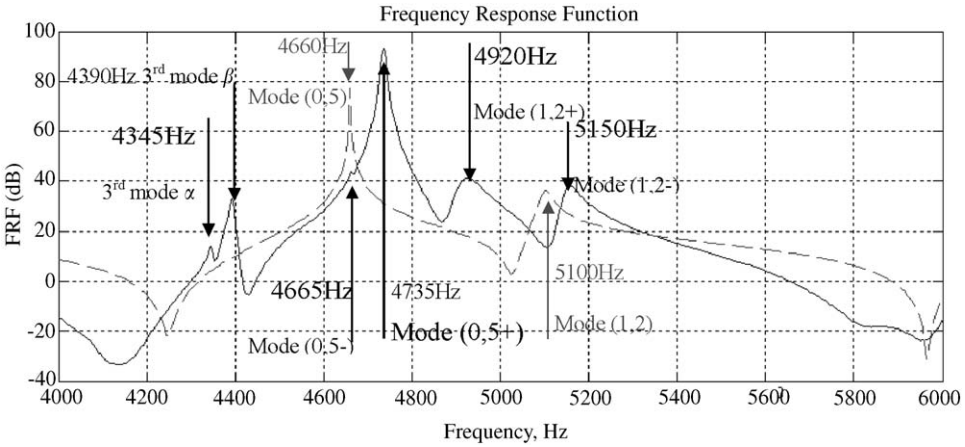

Fig. 4. Frequency response function: detail.

- the modes of the coupled system that correspond to either beam have higher frequencies than the corresponding uncoupled beam modes.

Since the two beams used here have the same dimensions and very similar boundary conditions, for each mode of the beams the laboratory brake presents two close eigenfrequencies, in a manner similar to mode splitting. In the present case, the lower frequency peak of the pair is associated with their out-of-phase motion, and the higher frequency corresponds to the in-phase motion of the beams.

We use the following notation to label the coupled system modes:

- mode $(n,m-)$: a nodal diameter is coincident with the contact point. At these frequencies the disc has a larger response than the beams;
- mode $(n,m+)$: an antinode is coincident with the contact point. At these frequencies the disc has a larger response than the beams;
- beam mode α: the two beams move out of phase; the beams have a larger response than the disc;
- beam mode β: the two beams move in phase; the beams have a larger response than the disc.

Fig. 3 shows an FRF of the coupled system, while Fig. 4 shows details of this coupled FRF between 4000 and 6000 Hz, along with the FRF of the uncoupled disc.

This frequency range contains the third mode of the uncoupled beam, at 4260 Hz, and the (0,5) and (1,2) modes of the uncoupled disc, at 4660 and 5100 Hz, respectively.

Under increasing contact force the beam modes shift toward higher frequencies and separate into the α and β modes at 4345 and 4390 Hz, respectively. The (0,5) mode of the disc (at 4660 Hz under uncoupled conditions) splits into the $(0,5-)$ and the $(0,5+)$ modes: the first one practically does not shift and remains at 4665 Hz, the second one shifts to 4735 Hz (Fig. 6A).

The measured deformed shapes (Fig. 5A and B) show that the β modes of the beam interact with the disc vibrations more than the α modes, while Figs. 5(C) and 6(A) show that the $(0,n+)$ mode interacts with the beam modes more than the $(0,n-)$ mode does (Fig. 6).

The (1,2) mode (Fig. 6B,C) behaves differently: the nodal diameter of the mode pair (1,2) does not cross the contact point, probably due to the presence of a close torsional mode of the beam. The $(1,2+)$ mode shifts toward a lower frequency and as a result splits -230 Hz.

Table 3 summarizes the coupled system behavior and shows the comparison between the frequencies of the uncoupled beam and the disc, and the natural frequencies of the coupled system for all the modes in the measurement range.

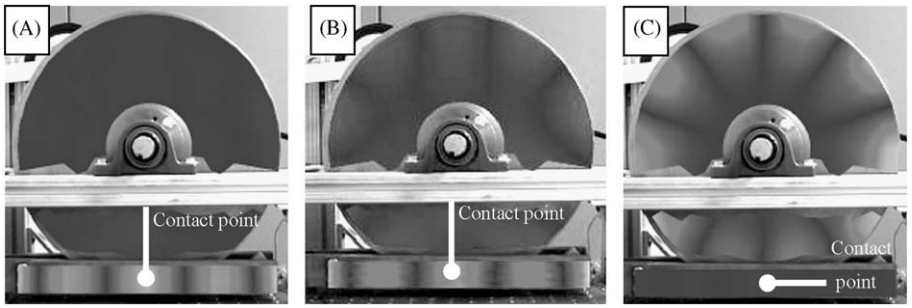

Fig. 5. Operative deformed shapes of the coupled system: (A) 3rd mode α of the beams, (B) 3rd mode β of the beams, (C) mode (0,5−).

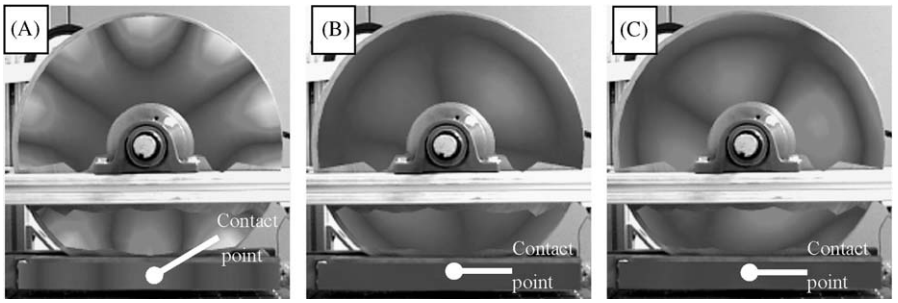

Fig. 6. Operative deformed shapes of the coupled system: (A) mode (0,5+), (B) mode (1,2−), (C) mode (1,2+).

Table 3
Comparison between coupled and coupled modes

Uncoupled mode	Frequency	Coupled mode	Frequency	Difference	Split
(0,1+)	709	(0,1)&rigid	470	−239	NA
(0,2)	845	(0,2)	845	0	
		(0,2+)&1st	1373	528	
First (beam)	877	First (beam)	1232	355	
(0,0)	1010	(0,0)&1st	967	−43	
(0,3)	1823	(0,3)	1828	5	182
		(0,3+)	2010	187	
Second (beam)	2180	Second (beam)	2260	80	
(1,1)	2612	(1,1)	2585	−27	120
(1,1+)	2846	(1,1+)	2683	−163	
(0,4)	3114	(0,4)	3118	4	85
		(0,4+)	3203	89	
(1,0)	3467	NA	NA	NA	
Third (beam)	4260	Third α (beam)	4345	88	
		Third β (beam)	4390	130	
(0,5)	4660	(0,5)	4665	5	70
		(0,5+)	4735	75	
(1,2)	5100	(1,2)	5150	50	−230
		(1,2+)	4920	−180	
(0,6)	6426	(0,6)	6430	4	45
		(0,6+)	6475	49	
(1,3)	7174	(1,3+)	7192	18	
(0,7)	8378	(0,7)	8383	5	32
		(0,7+)	8415	37	
(1,4)	9541	(1,4)	9545	4	

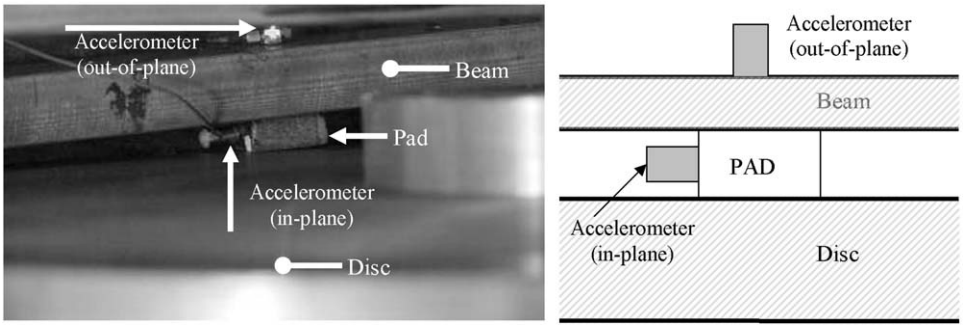

Fig. 7. Instrumentation for the evaluation of the in-plane dynamic of the pad.

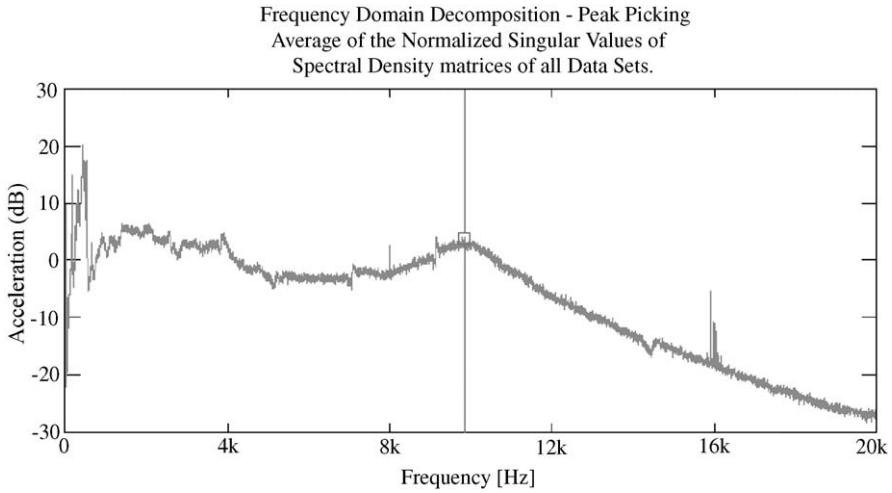

Fig. 8. Frequency domain decomposition.

The complete characterization of the coupled system should include the brake pad behavior. The pads also act as a critical bridge that connects the in- and out-of-plane dynamics of the disc and the beams: such interaction between in and out-of plane vibrations appears to be a key factor in squeal generation.

The results presented in Ref. [25] show that in the out-of-plane direction the pads act as a spring that connects the disc to the beam. The magnitude of their stiffness is a function of the normal load and increases with the load.

An "output only" modal identification method [26] based on the singular value decomposition is used to obtain information on the dynamic behavior of the pad in the in-plane direction. Fig. 7 shows a top view of the setup with an accelerometer mounted on the pad with its axis parallel to the direction of sliding. Rotating the disc excites the pad vibrations in a wide range of frequencies providing the natural excitation needed by the output only method.

Fig. 8 shows the frequency domain decomposition obtained by the software Art&mis. The plot shows that the pad has a rich content at low frequencies and presents a highly damped mode around 10 kHz, which is the only peak present in the frequency range of interest for the squeal phenomenon.

3. Characterization of the squeal behavior

This section describes the observed squeal behavior of the laboratory brake and highlights its main characteristics.

The conditions under which squeal developed were identified by rotating the disc at speeds between 5 and 30 rpm and adjusting the normal load and the geometrical configuration until an audible squeal sound was

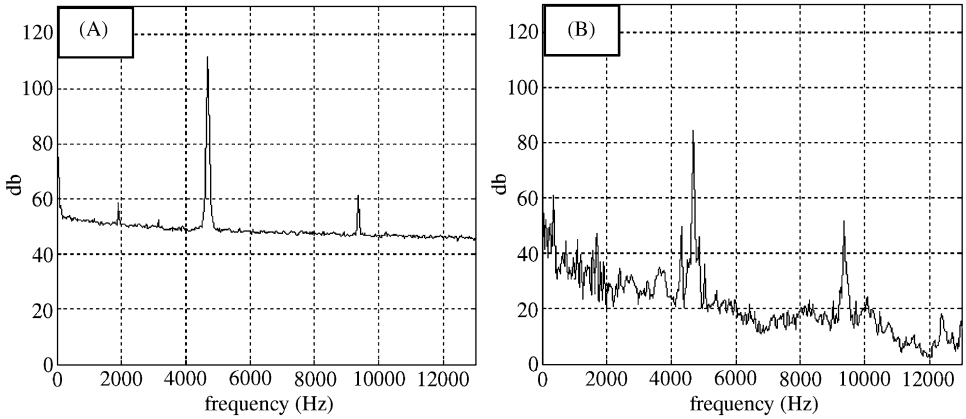

Fig. 9. Power spectral density of disc bending velocity (A) and sound pressure level (B) during squeal emission.

emitted. The same process was applied in searching for different conditions by changing the configuration of the setup.

In Section 3.1, a summary of general squeal characteristics observed during experiment are presented. The following subsections describe the correlation between squeal and several operational and dynamic parameters.

The squeal sounds observed usually have a periodic spectrum with the magnitude of the fundamental frequency higher than its sub-harmonics by 20–80 dB, depending on the test conditions. The fundamental frequency is always close to a natural frequency of the coupled system. As a result, the vibration response of the system is nearly identical to the corresponding mode-shape, which can be measured with the laser scanner.

Fig. 9 shows the power spectral density of the disc vibration velocity close to the contact point acquired during the squeal emission, obtained with the laser vibrometer, and of the emitted sound recorded with a microphone in the near field.

To measure the deformed shape of the system during squeal, a laser scan is performed.[5] The reference signal required for the laser vibrometer is provided by an accelerometer placed on the beam.

3.1. Summary of observed squeal characteristics

The acquisition parameters are set to have a very fast scan (32 kHz sampling frequency, and 200 FFT lines) of the surface, thus assuring that the squeal condition is constant during the measurement. The complete scan takes 25 s. The tradeoff is the reduction in frequency resolution of the measurement: however, since we are interested only in a small frequency band, this does not compromise the measurements. The squeal frequency, if needed with higher precision, can always be evaluated in the time domain.

By adjusting any of the parameters of the setup, such as the normal load, the geometrical configuration of the setup or the rotational speed of the disc, the squeal condition can:

- shift a few hertz, while maintaining the same deformed shape, with either an increase or a decrease in the sound amplitude;
- disappear completely, leaving only background vibration generated by the motor and the friction between disc and pad;
- shift to another squeal condition characterized by a completely different frequency and deformed shape.

Table 4 summarizes the squeal events occurred during tests.

[5]See Appendix A, Table A1 for the parameters used for the acquisition.

Fig. 10 shows the FRF of the coupled system at the drive point and the squeal frequencies (stars). All the squeal frequencies are close to one of the modes of the coupled system.

Fig. 11 shows the deformed shapes of the system during the squeal, measured with the laser scanner vibrometer: at 1920 Hz, involving the (0,4+) mode of the disc, at 4300 Hz, involving the 3rd mode of the beam, and at 8400 Hz, involving the (0,7+) mode of the disc.

The nodal lines of the disc during squeal become stationary in space due to the contact force. All the squealing conditions that involve primarily the disc develop at an $(n,m+)$ mode.

Table 4
Squeal frequencies

Frequency (Hz)	Mode
1920	(0,3+)
3100	(0,4+)
4300	Third beam
4700	(0,5+)
6400	(0,6+)
8400	(0,7+)
9480	Fifth beam
10,400	(0,8+)
12,400	(0,9+)

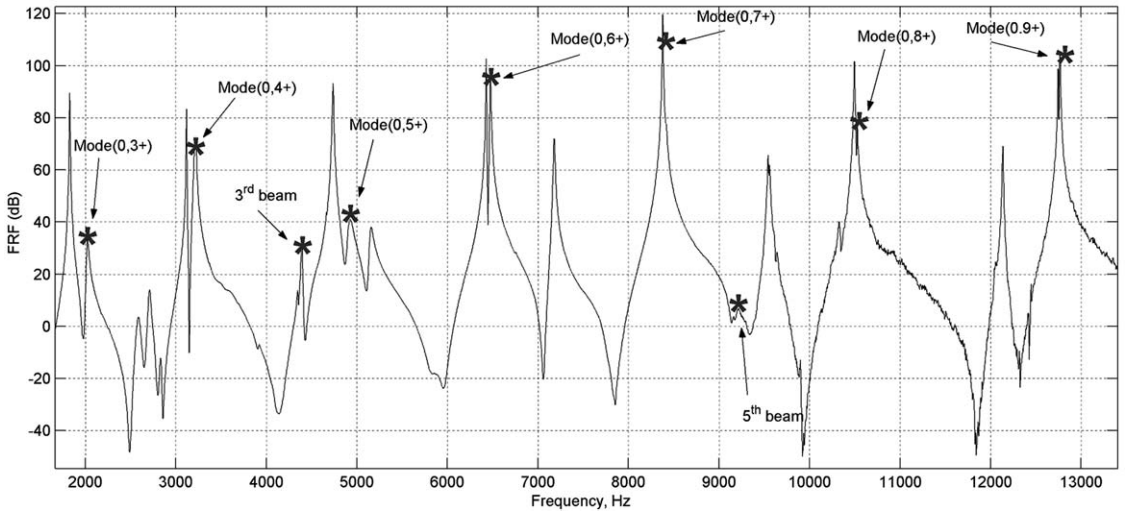

Fig. 10. FRF of the coupled system and squeal frequencies.

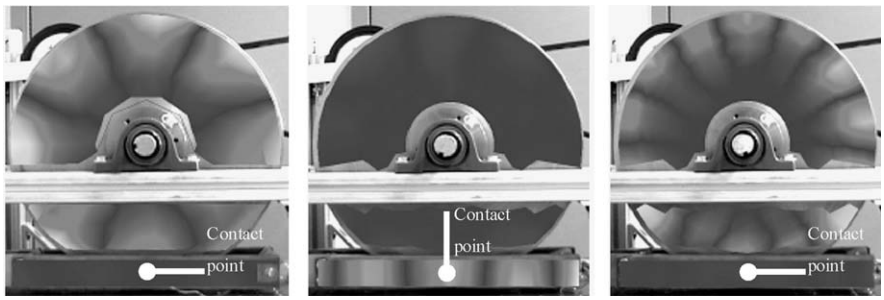

Fig. 11. Squeal deformed shapes.

Table 5
Squeal frequency (Laboratory brake V2.2)

Squeal frequency (kHz)	Mode
3.5	(0,4+) disc's mode
4.4	Third mode of the beam
5.3	(0,5+) disc's mode

The squeal conditions which primarily involve the beam have the two beams moving in-phase with very little disc vibrations at the contact point. Under these conditions, characterized by the β mode squealing, the disc at the contact point vibrates out of phase with the beams.

The results highlight that the highest propensity of squeal is obtained for modes characterized by a high relative displacement at the contact point.

3.2. Squeal and normal load

The tests for the characterization of the normal load-squeal frequency dependence were performed on the Laboratory brake V2.2.

Table 5 shows the squeal frequencies occurred on this setup.

The instrumentation used for the tests consists of two accelerometers, one on each beam, that provide the measurement of the acceleration signals and two load cells that measure the normal load. For each squeal condition a set of measurements is performed by changing the normal load in the range between 10 and 350 N. If the squeal sound emission is over 60 dB, the acquisition starts.[6]

A short acquisition (0.1024 s) assures that the characteristics of the squeal do not change during acquisition. To evaluate the squeal frequency with the needed resolution, a (time domain) identification of the main harmonics of the signals from the accelerometers is performed. During the tests the rotational velocity of the disc is set to 10 rpm.

The results, plotted in Fig. 12, show that for each squeal cluster there is a specific range of normal loads within which the system becomes unstable. The limit of this range depends on other secondary parameters such as the relative velocity or the generic configuration of the setup. In any case, it is evident that a very low level of normal load does not permit generation of squeal, and above a certain level the squeal stops. Each squeal cluster is characterized by a frequency which increases linearly with the normal load. Fig. 15 also shows a tendency for higher frequency squeal to develop at higher normal loads.

3.3. Squeal and angle of attack

Tests to qualify the dependency of the squeal frequency on the angle of attack of the pads were performed on both versions of the laboratory brakes V2.3 and V2.4.

During these tests the rotating speed was set to 10 rpm and the normal load to 200 N.

The angle of attack was adjusted until a squeal condition with a sound emission above 60 dB was reached; then a short acquisition started.[7]

The squeal frequency is evaluated in the time domain. To obtain a desired frequency resolution within such a short acquisition, the acquired signal is curve fitted with a sine signal; after each acquisition the angle is slightly changed and another acquisition is performed.

The acquired signals include the out-of-plane acceleration of the beam, the vibration velocity of the disc close to the contact point with the laser vibrometer, and the sound pressure measured with a condenser microphone.

[6]See Appendix A, Table A2, for the acquisition parameters.
[7]See Appendix A, Table A2 for the acquisition parameters.

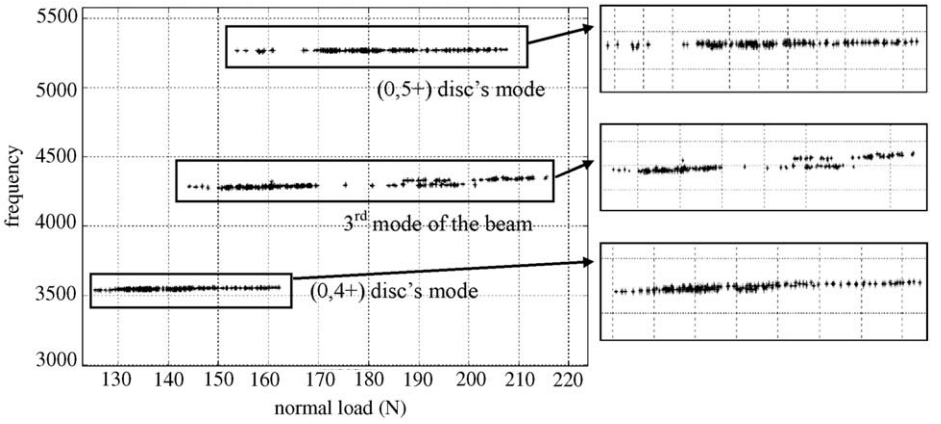

Fig. 12. Squeal frequency vs. normal load.

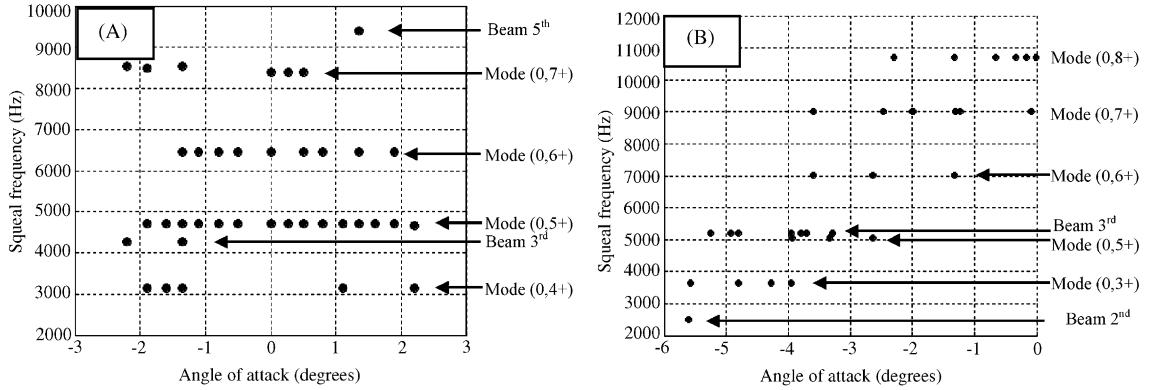

Fig. 13. Squeal frequency as a function of the angle of attack: (A) Lab-brake V2.3, (B) Lab-brake V2.4.

Fig. 13 shows the results from the tests performed on the laboratory brake V.2.3 for negative angles of attack and on the V.2.4 with the angle ranging from -3° to 3°. The figure shows a general tendency for higher frequency squeal to develop for angles of attack close to zero.

It is important to note here that the squeal frequencies are influenced by many parameters other than the angle of attack, such as the normal load and the wear of the surfaces in contact. The wear in particular is a parameter that is hard to control and may contribute to the high level of dispersion of data.

3.4. Squeal and pad dynamics

To characterize the behavior of the setup and to understand how the components of the system vibrate during squeal emission, phase relationships between the pads are investigated. Using two accelerometers on each pad, one to measure in-plane and the other to measure the out-of-plane response, simultaneous recording of accelerations were made during squeals. The accelerometers to measure the out-of-plane vibrations of the pads were mounted on the beams opposite the pad as shown in Fig. 7.[8] The time-domain analysis of the acceleration response of the pads during squeal shows that, during each squeal, at least one of the pads has an in-plane acceleration approximately 90° out of phase with respect to its out-of-plane response. This effect was also highlighted by Ichiba et al. [27].

[8]See Appendix A, Table A2 for the acquisition parameters.

Fig. 14 shows the out-of-plane direction (continuous line) and the in-plane direction (dashed line) accelerations measured during a squeal emission; each of these measurements relates to the squeals that develop in the laboratory brake V2.2. at 3.5, 4.4, and 5.3 kHz, respectively.

The measurements show that squeal emission is always associated with either one or both of the pads each having a 90° phase difference between in-plane and out-of-plane acceleration response.

In cases when only one pad has 90° phase difference, the significance of this phase relationship was investigated by disturbing the in-plane dynamics of the pad that showed a 90° phase difference by simply applying pressure to it by softly touching the pad in the in-plane direction with the tip of a screwdriver. As shown in Figs. 15 and 16, application of a light pressure to this pad immediately stops the squeal, and its removal initiates the squeal again, while similar alteration of the in-plane dynamic of the other pad has a little effect on the emitted sound; the squeal just reduces its amplitude but it does not stop at all.

It is important to note that when squeal starts, the squeal behavior is highly robust, except for in-plane dynamics of the squeal inducing pad. In fact, even strong changes in the setup parameters (e.g. increasing the damping by grabbing the disc with two hands while it is rotating at low rpm) do not stop the squeal.

These simple tests show that squeal can occur either when one or both pads induce instabilities (as indicated by a 90° phase difference). Thus, altering the in-plane behavior of the unstable pads stops the squeal.

It is important to also note that the squeal is sensitive only to in-plane changes; in fact, applying light pressure to the squealing pad in the normal direction does not stop squeal.

Further measurements presented below address the influence of additional parameters on squeal development, such as wear, on squeal development.

For example, when a new set of pads is used, generally it is hard to obtain a squeal event. However, after a few minutes of running-in, the system starts to produce squeal sounds over a wide range of frequencies,

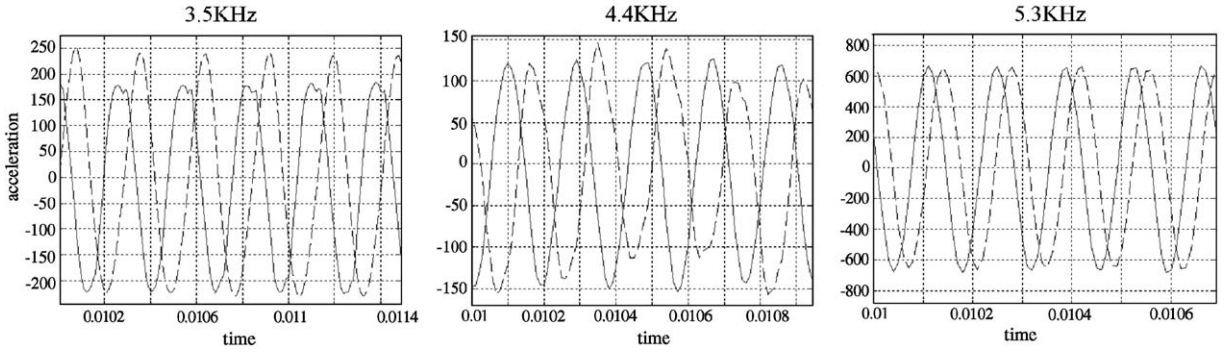

Fig. 14. In-plane (dashed) and out-of-plane (continuous) acceleration of the pad.

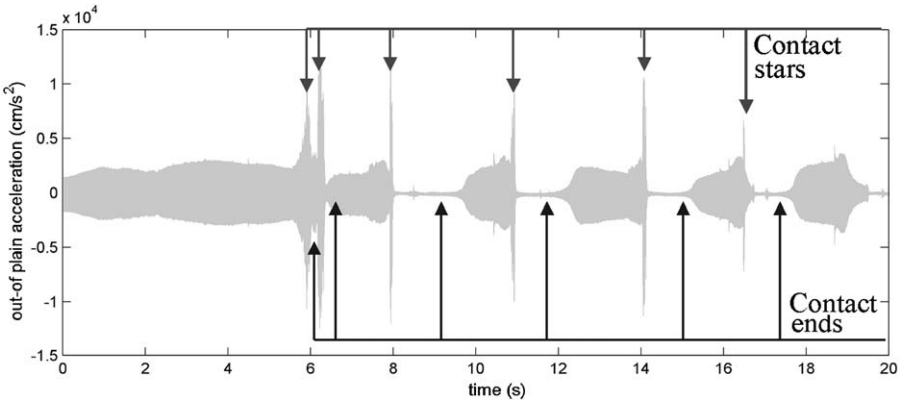

Fig. 15. Alteration of the in-plane behavior of pad: pad with phase difference.

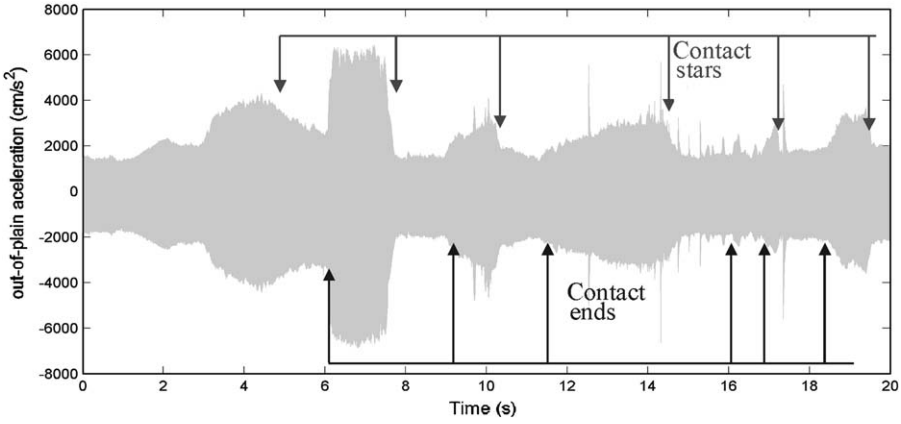

Fig. 16. Alteration of the in-plane behavior of pad: pad without phase difference.

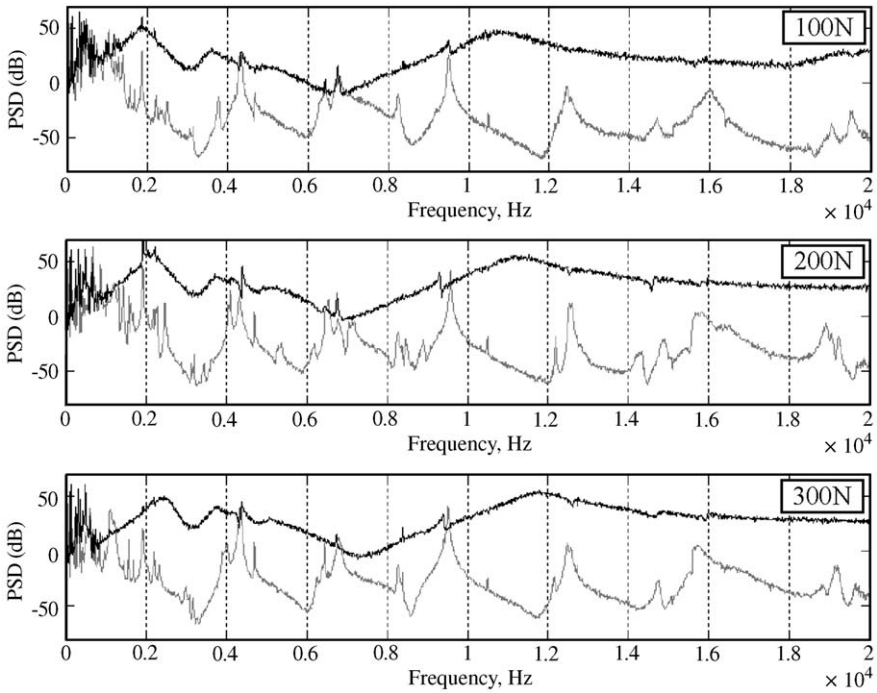

Fig. 17. PSD of the pad: in-plane (black), out-of-plane (gray). After 100 cycles.

generally between 1 and 7 kHz, and it is quite easy to change the squealing mode by adjusting the normal load or the angle of the beams. After a while the system starts to produce squeal only in a small range of frequencies, usually between 8 and 11 kHz and it is no longer possible to obtain squeal at low frequencies.

Figs. 17 and 18 each presents three sets of power spectral density measurements for the in-plane and out-of-plane vibrations of one of the pads. These measurements are made after 100 and 1000 cycles following insertion of new pads, to investigate the changing squeal conditions with time. In all cases, the disc rotation speed was kept at 10 rpm for normal loads of 100, 200, and 300 N. Squeal started to develop after 100 cycles of rotation and involved the (0,3 +) (0,4 +) (0,5 +) modes of the disc or the 3rd mode of the beam at 1920, 3100, 4700, and 4300 Hz, respectively.

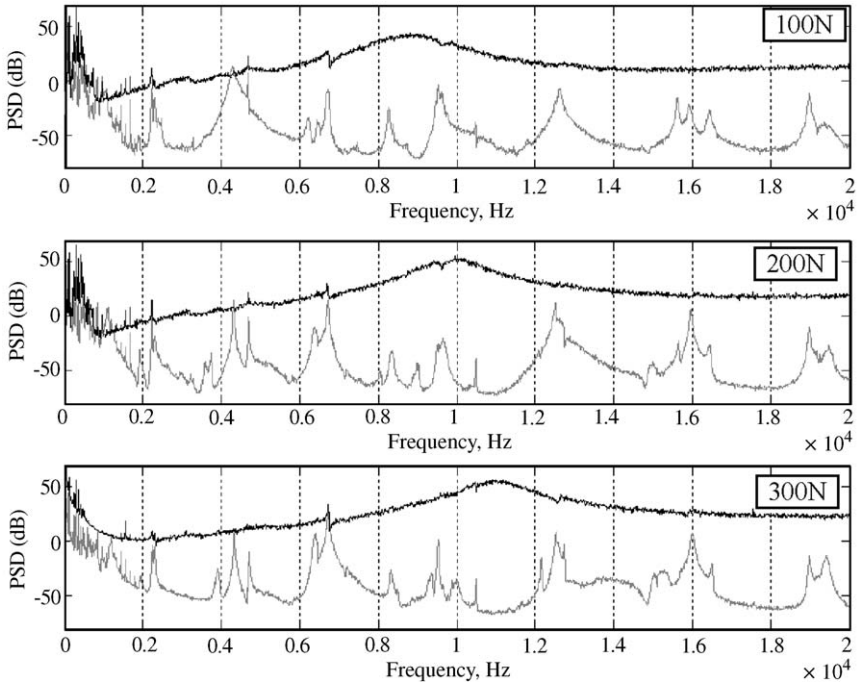

Fig. 18. PSD of the pad: in-plane (black), out-of-plane (gray). After 1000 cycles.

The out-of-plane response (gray line) in Fig. 17 contains all the system frequencies excited during squeal. The in-plane response of the pad (dark line) also exhibits some of the same frequencies but less prominently than the out-of-plane response. In addition, however, the in-plane response contains highly damped spectral peaks at 2, 3.5, 4.5 and 11 kHz. The frequencies of these peaks increase with normal load as shown in Fig. 17, while those associated with system frequencies that dominate the out-of-plane response do not change significantly.

After 1000 cycles of disc rotation, squeal develops only at 9100 Hz, involving 5th mode of the beam, and at 10.5 and 12.8 kHz, involving the (0,8 +) and the (0,9 +) modes of the disc, respectively. After 1000 cycles, only a highly damped peak at 10 kHz dominates the in-plane response of the pads at 100 N normal load and increases with increasing normal load.

These results suggest for the following explanation of the mechanism of selection of the squealing mode.

The squeal occurs at an out-of-plane eigenfrequency of the coupled system that is close to one of the in-plane eigenfrequencies of the pad.

Such consideration is also consistent with the previously mentioned squeal characteristics i.e.:

- a 90° phase shift, caused by the resonance of the in-plane mode on the pad, between the in-plane and out-of plane eigenfrequency of the pad;
- a high sensitivity of the squeal event to the in-plane dynamics of the pad.

Finally, the tendency for higher frequency squeal, developed under increasing normal load, can be correlated to the increase of the in-plane eigenfrequency of the pad with increasing normal load.

3.5. Squeal and relative velocity

The following measurements describe any dependence of the squeal characteristics on the relative velocity between disc and pad and also investigate whether stick-slip develops during squeal emission.

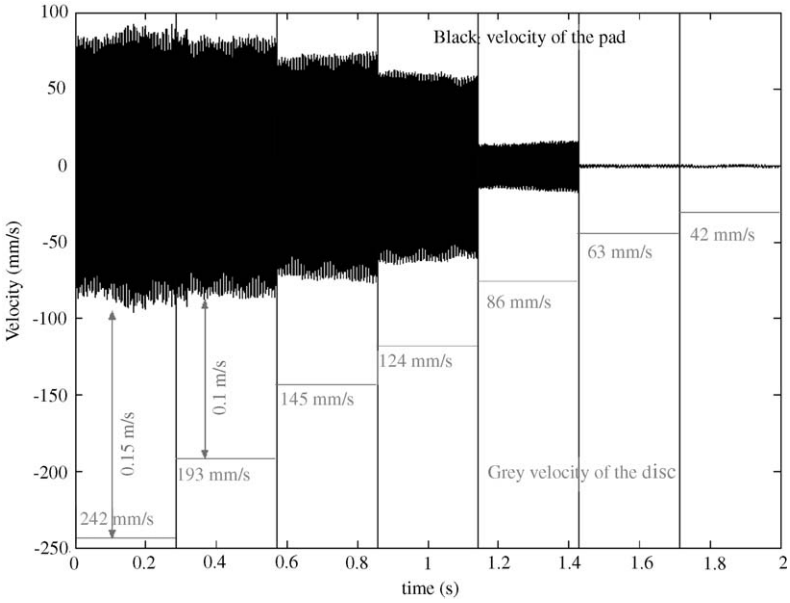

Fig. 19. Relative velocity between disc and pad.

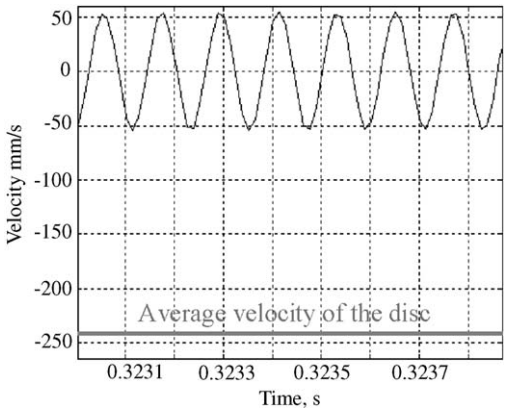

Fig. 20. Relative velocity: detail.

Measurement of the in-plane velocity of the pad by a laser vibrometer close to its contact surface and of the average velocity of the disc obtained using a digital encoder produced the relative velocity between the pad and disc. Two accelerometers provided reference signals and characterized the beams vibration.[9]

The measurements reported in Fig. 19 follow the squeal at 10.4 kHz that involves primarily the (0,8 +) mode of the system under a normal load of 200 N. Since due to run-outs on the disc surface squeals may develop only during part of a cycle, measurements are locked into the same angular position of the disc, for each of the seven cases reported for different rotational speeds ranging from 242 to 42 mm/s.

The results show that the average velocity of the disc is always higher than the maximum in-plane vibration velocity of the pad. As shown in detail in Fig. 20, the margin between the two is always large enough to assure that neither irregularity in the rotation of the disc nor errors due to the distance between the measurement point where laser is focused on and the effective contact point (the distance is less than a millimeter) may cause a change of direction in the relative velocity.

[9]See Appendix A, Table A2 for the acquisition parameters.

The measurements also showed an insensitivity of sound pressure amplitude to speed at the higher end of the rotational speeds tested (above 200 mm/s). At lower speeds, below 60 mm/s, squeal disappeared. In the range between 60 and 200 mm/s sound pressure amplitude decreased with decreasing rotational speed of the disc.

Further measurements would be necessary to completely characterize the dependence of squeal amplitude on the relative velocity.

4. Conclusions

The breadth of squeal conditions it can generate with repeatability makes the laboratory brake a useful tool to investigate brake squeal sounds. Its ability to selectively provide the different coupling strengths among the components, pad and disc in particular, enables correlation of dynamic response of the system and its components to squeal generation, making it a useful design tool.

The results produced using the laboratory brake can be summarized as follows:

- squeal occurs at frequencies close to natural frequencies of the coupled system;
- squeals primarily involving a particular disc mode occur at the second peak of a split mode; therefore such squeals from the laboratory brake involve the $(n,m+)$ modes;
- squeal involving a beam mode generally occurs at the frequency of the so-called β mode;
- squeal frequency within a squeal cluster increases with normal load as a result of stiffening the system modes. Squeal clusters at higher frequencies develop under higher normal loads;
- squeals are characterized by a 90° phase difference between the in-plane and the out-of-plane accelerations of the pad. The in-plane motion of the pad leads that of the out-of-plane;
- the in-plane dynamics of the pad plays a key role in the squeal mode selection, i.e. squeal frequencies occur at frequencies close to one of the natural frequencies of the pad vibration in the in-plane direction;
- squeal does not require that a stick-slip limit cycle is established;
- squeal frequency is not globally affected by changes in relative velocity.
- The vibration modes in the disc during squeal events are all fixed in space. In fact, the considered configuration of the setup is not capable of producing rotating squeal as reported sometimes in literature. However, another configuration of the laboratory brake, that has pads of larger dimension [28], or using two pads attached to each beam [29], can produce rotating squeal events.

Capability to produce such set of results that can be reproduced at will on a single experimental rig, can be useful to build predictive models of the squeal behavior of the setup.

The instability mechanism that develops in the laboratory brake can be summarized as follows: the friction force couples the bending vibrations of the laboratory brake and the in-plane vibration of the pad; the friction force is in-phase with the relative displacement between the disc and the pad. If the system vibrates with a frequency close to a natural frequency of the pad, i.e. if a natural frequency of the system falls close to an in-plane eigenfrequency of the pad, the pad vibrates with a 90° phase difference with respect to the bending vibration of the disc and the beams. This implies an elliptic trajectory of the contact point on the pad that can transfer energy from the continuous rotation of the disc to the vibrational motion of the pad.

Many other aspects of squeal phenomenon need further investigation and further experimental work should be devoted to better characterization of the nonlinear aspects of contact between the disc and the pad, especially the dependence between wear and the in-plane eigenfrequency of the pad. Measurements show that there is not a global stick-slip motion during the squeal occurrence. Moreover, the complexity of the setup should be increased to study the high-frequency squeal with an extended contact area between disc and pad to bring the setup design closer to that of a brake.

Finally, in order to find a solution to the squeal problem, it would be still necessary to develop an experimental benchmark of brake, characterized by a well defined geometry and standardized contact conditions. Such benchmark would permit comparisons of experimental and numerical results obtained by different groups and test them on a standard platform. The laboratory brake could be a good choice for such benchmark.

Appendix A

Tables A1 and A2 show the parameters used for the acquisition.

Table A1
Laser scanner acquisition parameters

	Retrieval of the dynamical behaviour of the coupled system	Squeal deformed shape measure
Scan points	301	301
Averaging	Complex	Complex
FFT lines	6400	200
Resolution	1.953 Hz	80 Hz
Valid points	100%	100%
Averaging count	3	3
Sample frequency	32 kHz	32 kHz
Window	Rectangular	Rectangular
Acquisition mode	FFT	FFT
Bandwidth	12.5 kHz	12.5 kHz
Sample time	0.512s	0.0125s
Tracking filter	Fast	Fast

Table A2
Acquisition parameters

	Squeal normal load tests	Squeal angle tests	Squeal and pad dynamics tests	Squeal and relative velocity tests
Sample freq.	40 kHz	40 kHz	40 kHz	40 kHz
No. of channel	5	5	5	5
No. of sample	4096	4096	2106	2106
Freq. resolution	9.76 Hz	9.76 Hz	NA	NA
Acquisition time	0.1024s	0.1024s	50s	50s
Low pass filter	15000 Hz	15000 Hz	15000 Hz	15000 Hz

References

[1] N.M. Kinkaid, O.M. O'Reilly, P. Papadopoulos, Automotive disc brake squeal, *Journal of Sound and Vibration* 267 (2003) 105–166.
[2] H.R. Mills, Brake squeak, Technical Report 9000 B, Institution of Automobile Engineers, 1938.
[3] R.A.C. Fosberry, Z. Holubecki, Interim report on disc brake squeal, Technical Report 1959/4, Motor Industry Research Association, Warwickshire, England, 1959.
[4] R.A.C. Fosberry, Z. Holubecki, Disc brake squeal: its mechanism and suppression, Technical Report 1961/1, Motor Industry Research Association, Warwickshire, England, 1961.
[5] R.T. Spurr, A theory of brake squeal, in: *Proceedings of the Automobile Division*, Institution of Mechanical Engineers, 1961–1962, No. (1), 1961, pp. 33–52.
[6] M.R. North, Disc brake squeal, a theoretical model, Technical Report 1972/5, Motor Industry Research Association, Warwickshire, England, 1972.
[7] M. Nishiwaki, H. Harada, H. Okamura, T. Ikeuchi, Study on disc brake squeal, Technical Report 890864, SAE, Warrendale, PA, 1989.
[8] J.D. Fieldhouse, P. Newcomb, The application of holographic interferometry to the study of disc brake noise, Technical Report 930805, SAE, Warrendale, PA, 1993.
[9] J.D. Fieldhouse, T.P. Newcomb, Double pulsed holography used to investigate noisy brakes, *Optics and Lasers in Engineering* 25 (6) (1996) 455–494.

[10] Y. Denou, M. Nishiwaki, First order analysis of low frequency disk brake squeal, Technical Report 2001-01-3136, SAE, Warrendale, PA, 2001.
[11] S.W.E. Earles, G.B. Soar, Squeal noise in disc brakes, in: *Vibration and Noise in Motor Vehicles*, Institution of Mechanical Engineers, London, England, 1971, pp. 61–69 (Paper number C 101/71).
[12] S.W.E. Earles, A mechanism of disc-brake squeal, Technical Report 770181, SAE, Warrendale, PA, 1977.
[13] R.P. Jarvis, B. Mills, Vibrations induced by friction, *Proceedings of the Institution of Mechanical Engineers* 178 (32) (1963) 847–857.
[14] M.R. North, Disc brake squeal, in: *Braking of Road Vehicles, Automobile Division of the Institution of Mechanical Engineers*, Mechanical Engineering Publications Limited, London, England, 1976, pp. 169–176.
[15] K. Popp, P. Stelter, Stick-slip vibrations and chaos, *Philosophical Transactions on the Royal Society of London A* 332 (1990) 89–105.
[16] M. Rudolph, K. Popp, Friction induce brake vibration, in: *Proceedings of DETC'01*, VIB21509, Pittsburgh, PA, 2001.
[17] J.E. Mottershead, Vibration- and friction-induced instability in disks, *Shock and Vibration Digest* 30 (1) (1998) 14–31.
[18] S.N. Chan, J.E. Mottershead, M.P. Cartmell, Parametric resonances at subcritical speeds in discs with rotating frictional loads, *Proceedings of the Institution of Mechanical Engineers Part C* 208 (C6) (1994) 417–425.
[19] A. Akay, J. Wickert, Z. Xu, Investigation of mode lock-in and friction interface, Final Report, Department of Mechanical Engineering, Carnegie Mellon University, 2000.
[20] A. Tuchinda, N.P. Hoffmann, D.J. Ewins, W. Keiper, Effect of pin finite width on instability of pin-on-disc systems, in: *Proceedings of the International Modal Analysis Conference—IMAC*, Vol. 1, 2002, pp. 552–557.
[21] A. Tuchinda, N.P. Hoffmann, D.J. Ewins, W. Keiper, Mode lock-in characteristics and instability study of the pin-on-disc system, in: *Proceedings of the International Modal Analysis Conference—IMAC*, Vol. 1, 2001, pp. 71–77.
[22] R. Allgaier, L. Gaul, W. Keiper, K. Willnery, N. Hoffmann, A study on brake squeal using a beam on disc, in: *Proceedings of the International Modal Analysis Conference—IMAC*, Vol. 1, 2002, pp. 528–534.
[23] R. Allgaier, Experimentelle und numerische untersuchungen zum bremsenquietschen, Ph.D. Thesys, University of Stuttgart, reihe12 Nr481.
[24] J.F. Tarter, Instabilities in a beam-disc system due to friction, Ph.D. Thesis, Carnagie Mellon University, 2004.
[25] O. Giannini, Experiments and modeling of squeal noise on a laboratory disc brake, Ph.D. Thesis, University of Rome "La Sapienza", 2004.
[26] R. Brincker, L. Zhang, P. Andersen, Modal identification of output-only systems using frequency domain decomposition, in: *Proceedings of the European COST F3 Conference on System Identification and Structural Health Monitoring*, Madrid (Spain), 2000.
[27] Y. Ichiba, Y. Nagasawa, Experimental study on brake squeal, Technical Report 930802, SAE, Warrendale, PA, 1993.
[28] F. Massi, O. Giannini, Extension of a modal instability theory to real brake systems, in: *Proceedings of IMAC XXIII Paper No. 91*, Orlando, FL, February 2005.
[29] O. Giannini, F. Massi, A. Sestieri, Experimental characterization of the high frequency squeal on a laboratory brake set-up, in: *Proceedings of IMAC XXIII Paper No. 107*, Orlando, FL, February 2005.